ADVANCED SENSOR RESEARCH Open Access
www.advsensorres.com

Highly Reusable Electrochemical Immunosensor for Ultrasensitive Protein Detection

Kavya L. Singampalli, Camille Neal – Harris, Cassian Yee, Jamie S. Lin, and Peter B. Lillehoj**

The detection and quantification of protein biomarkers in bodily fluids is important for many clinical applications, including disease diagnosis and health monitoring. Current techniques for ultrasensitive protein detection, such as enzyme-linked immunosorbent assay (ELISA) and electrochemical sensing, involve long incubation times (1.5–3 h) and rely on single-use sensing electrodes which can be costly and generate excessive waste. This work demonstrates a reusable electrochemical immunosensor employing magnetic nanoparticles (MNPs) and dually labeled gold nanoparticles (AuNPs) for ultrasensitive measurements of protein biomarkers. As proof of concept, this platform is used to detect C-X-C motif chemokine ligand 9 (CXCL9), a biomarker associated with kidney transplant rejection, immune nephritis from checkpoint inhibitor therapy, and drug-associated acute interstitial nephritis, in human urine. The sensor successfully detects CXCL9 at concentrations as low as 27 pg mL^{-1} within ≈1 h. This immunosensor was also adapted onto a handheld smartphone-based diagnostic device and used for measurements of CXCL9, which exhibited a lower limit of detection of 65 pg mL^{-1}. Lastly, this work demonstrates that the sensing electrodes can be reused for at least 100 measurements with a negligible loss in analytical performance, reducing the costs and waste associated with electrochemical sensing.

1. Introduction

The detection and quantification of protein biomarkers play an important role in the diagnosis and monitoring of diseases. Enzyme-linked immunosorbent assay (ELISA) is the most commonly used immunological technique for the detection and quantification of proteins in biofluid samples.[1] While ELISA enables high sensitivity and high specificity measurements, it involves long (1.5–3 h) incubation times and requires bulky benchtop equipment and highly trained personnel, limiting its use to laboratory settings. Electrochemical sensing is an alternative technique capable of high sensitivity biomolecular detection, which can be performed using portable instrumentation.[2-4] Immunoassays employing electrochemical sensing (i.e., electrochemical immunosensors) have been integrated onto smartphone-based detection devices, facilitating their use for point-of-care testing.[5-7] However, electrochemical immunological techniques rely on the formation of antibody-antigen immunocomplexes, which can involve long incubation times similar to ELISA. Furthermore, electrochemical sensors utilize single-use sensing electrodes, which leads to higher costs and excessive waste.

Various strategies have been demonstrated to develop electrochemical sensing electrodes that can be reused for multiple measurements. One such method is to use shape-changing aptamers to reversibly bind the analyte under different conditions. Yang et al. developed an electrochemical sensor for the detection of

K. L. Singampalli, C. Neal – Harris, P. B. Lillehoj
Department of Bioengineering
Rice University
Houston, TX 77030, USA
E-mail: lillehoj@rice.edu

The ORCID identification number(s) for the author(s) of this article can be found under https://doi.org/10.1002/adsr.202400004

© 2024 The Authors. Advanced Sensor Research published by Wiley-VCH GmbH. This is an open access article under the terms of the Creative Commons Attribution License, which permits use, distribution and reproduction in any medium, provided the original work is properly cited.

DOI: 10.1002/adsr.202400004

K. L. Singampalli
Medical Scientist Training Program
Baylor College of Medicine
Houston, TX 77030, USA

C. Yee
Department of Melanoma Medical Oncology
UT MD Anderson Cancer Center
Houston, TX 77030, USA

J. S. Lin
Section of Nephrology, Division of Internal Medicine
UT MD Anderson Cancer Center
Houston, TX 77030, USA
E-mail: jlin8@mdanderson.org

P. B. Lillehoj
Department of Mechanical Engineering
Rice University
Houston, TX 77005, USA

carcinoembryonic antigen (CEA) in blood.[8] This platform utilized a tetrahedral DNA nanostructure on the surface of the working electrode, which formed a triplex structure in the presence of CEA, bringing a redox element close to the electrode surface. Rinsing the sensing electrodes using an alkali solution caused the nanostructure to return to its original configuration and release CEA, allowing it to be reused. This sensor could detect CEA at concentrations as low as 2 pM in 35 min and be reused up to 13 times with a <15% loss in the detection signal. Similarly, Wu et al. reported a reusable electrochemical sensor employing a ferrocene-bound aptamer for the detection of adenosine, which could be detected at concentrations as low as 20 nM.[9] Rinsing the sensing electrodes with hot water caused adenosine to be released from the aptamer, enabling the sensor to be reused up to 30 times while maintaining >90% of the detection signal.

Modifying the sensor surface to release immobilized proteins is another technique that has been implemented to reuse sensing electrodes. For example, Hong et al. coated a gold sensor in poly(N-isopropylacrylamide) to create a thermoresponsive layer on the surface of the sensing electrode.[10] At temperatures above 32 °C, hydrophobic interactions allowed the polymer to adsorb proteins for immunocomplex formation. This platform was used to detect cancer antigen 125, CEA, and prostate specific antigen (PSA), which could be detected at concentrations as low as 0.007 U mL^{-1}, 0.7 pg mL^{-1}, and 0.9 mg mL^{-1}, respectively. The target proteins could be released by reducing the temperature below 32 °C, allowing the sensing electrodes to be reused for up to 4 measurements without a drop in analytical performance. In an alternative method demonstrated by Panahi et al., the surface of an electrochemical sensor was modified with polyethylene glycol and cyclodextrin, which underwent a change in its polymeric confirmation in the presence of hydrophobic analytes, such as *trans*-resveratrol, leading to a drop in the electrochemical impedance.[11] Introducing cyclodextrins back into the polyethylene glycol surface restored the sensor functionality, allowing it to be reused for 3 measurements.

Another strategy that has been utilized to reuse sensing electrodes is to dissociate the antigen-antibody immunocomplexes from the sensor surface using an acidic solution, such as glycine-hydrochloric acid buffer,[12,13] or a solution containing a strong base, such as NaOH.[14] Using this approach, immunosensors could achieve high sensitivity detection when combined with signal amplification strategies[14] and be reused up to 45 times;[13] however, they required harsh chemicals or complicated washing procedures to remove bound analytes, limiting their use to laboratory settings. Sensing electrodes can also be reused by washing the electrode surfaces to remove whole antigen-antibody immunocomplexes and re-immobilizing the capture antibody. Zhang et al. developed a reusable amperometric immunosensor that could be reused up to four times by dissociating antibody-antigen immunocomplexes from the working electrode using a regeneration solution.[15] Using a similar sensing scheme and sensor regeneration principle, Liu et al. developed an amperometric immunosensor with a phenylboronic acid-modified working electrode for measurements of PSA, which could be detected at concentrations as low as 2 ng mL^{-1}, and reused up to 10 times.[16] While these immunosensors exhibited minimal variability (< 5% relative standard deviation) across measurements using reused electrodes, they required long soaking times (30 min) in the regeneration solution and the capture antibody needed to be re-immobilized on the working electrode after each measurement.

Magnetic beads have also been used to create reusable sensors, which enable the rapid immobilization and removal of immunocomplexes from the surface of an electrode. Xiao et al. reported a magnetic bead-based electrochemical sensing platform for the detection of *E. coli* in food samples.[17] An *E. coli*-specific antibody was immobilized onto magnetic beads and concentrated on the working electrode by placing the sensor on a magnet. Using this platform, *E. coli* could be detected at concentrations as low as 3 colony forming units. *E. coli*-bead complexes were removed from the working electrode via washing with ammonia and distilled water, allowing the sensing electrodes to be reused for up to 60 measurements.

Reusable piezoelectric and field-effect transistor (FET)-based biosensors have also been reported. For example, piezoelectric sensors have been developed that employ magnetic beads to immobilize the capture antibody on the sensor surface[18,19] or can be washed to dissociate antibody-antigen immunocomplexes from the sensing surface.[20–22] While some of these sensors could be reused up to 100 times, they required the capture antibody to be re-immobilized on the sensing surface after each measurement. Furthermore, these biosensors exhibited analytical sensitivities in the range of 10′s of ng mL^{-1}, making them unsuitable for the detection of many clinically relevant biomarkers that are present at low concentrations (10′s to 1000′s pg mL^{-1}) in bodily fluids. FET-based sensors have also been developed with various reusability strategies, including using sensor coatings with reversible protein binding properties,[23] modifying nano-FET sensing elements with polymers or peptides,[24–26] or utilizing aptamers with shape-transitioning properties as biorecognition elements.[27] While these platforms could be reused at least 10 times, the fabrication of FET-based sensors is complicated and expensive, limiting their use to research purposes.

To overcome the limitations described above, we have developed an electrochemical immunosensor for ultrasensitive (10′s pg mL^{-1}) protein measurements with excellent reusability. This immunosensor is based on a unique sensing scheme using antibody-labeled magnetic nanoparticles (MNPs) and gold nanoparticles (AuNPs), enabling rapid immunomagnetic enrichment and enhanced signal amplification. For proof of concept demonstration, we have selected C-X-C motif chemokine ligand 9 (CXCL9), which has been shown to be an important biomarker for the detection of immune nephritis associated with treatable medical conditions, such as renal transplant rejection[28–30] and acute interstitial nephritis from immune checkpoint inhibitors or other drugs.[31,32] The use of this immunosensor for the detection of CXCL9 in urine samples is novel and represents a pioneering application of this technology. We show the capability of this immunosensor to detect CXCL9 in spiked human urine samples with pg mL^{-1} sensitivity in ≈1 h. Furthermore, we also demonstrate CXCL9 detection using a smartphone-based diagnostic device, providing enhanced portability for point-of-care testing. Last, we show that sensing electrodes can be rinsed and reused for at least 100 measurements with a minimal loss in analytical performance.

© 2024 The Authors. Advanced Sensor Research published by Wiley-VCH GmbH

27511219, 0, Downloaded from https://onlinelibrary.wiley.com/doi/10.1002/adsr.202400004 by Rice University, Wiley Online Library on [22/04/2024]. See the Terms and Conditions (https://onlinelibrary.wiley.com/terms-and-conditions) on Wiley Online Library for rules of use; OA articles are governed by the applicable Creative Commons License

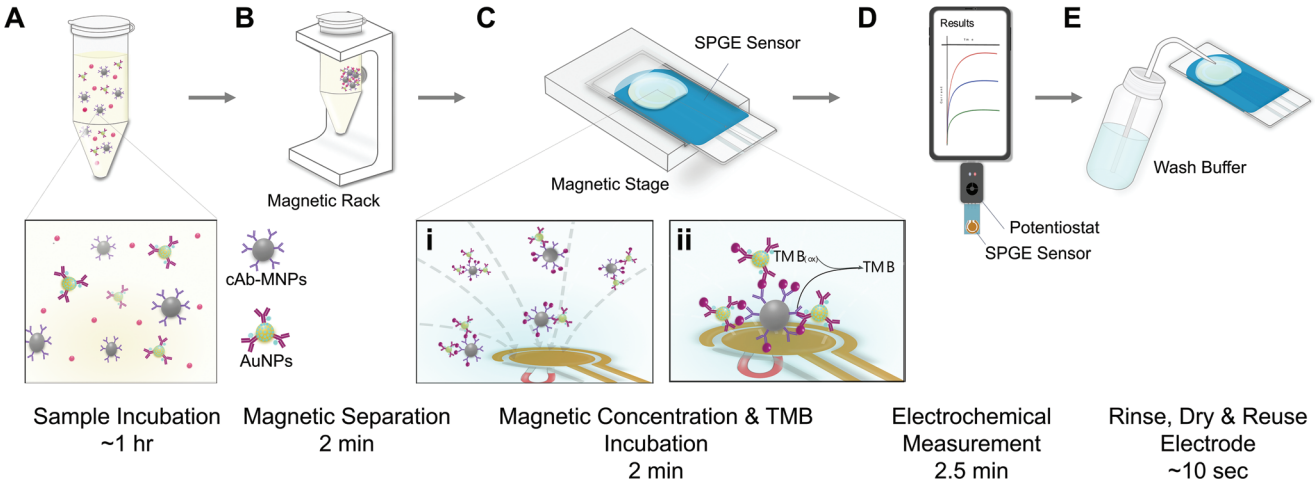

Figure 1. Workflow of the Reusable Electrochemical Immunosensor. A) The sample is incubated with cAb-MNPs and dually labeled AuNPs, resulting in the formation of MNP-antigen-AuNP immunocomplexes. B) MNP-antigen-AuNP immunocomplexes are separated from the sample using a magnetic rack. C) TMB substrate is added to the MNP-antigen-AuNP immunocomplexes and the solution is dispensed onto the SPGE sensor. The sensor is placed on a magnetic stage resulting in the MNP-antigen-AuNP immunocomplexes being concentrated onto the working electrode (i). A bias potential is applied to the reference and working electrodes, and an electrochemical current is generated by the HRP-TMB substrate redox reaction (ii). D) The electrochemical signal is read using a smartphone-based diagnostic device or a benchtop potentiostat. E) The sensor is gently rinsed with wash buffer and dried using compressed air, enabling it to be reused.

2. Results and Discussion

2.1. Principle of the Sensing Scheme

Unlike conventional antigen immunoassays that utilize a capture antibody that is permanently immobilized on the sensing surface and a horseradish peroxidase (HRP)-conjugated detection antibody, this immunosensor utilizes capture antibody-labeled (cAb-) MNPs and AuNPs dually labeled with a biotinylated detection antibody and HRP. To initiate the measurement, cAb-MNPs and dually labeled AuNPs are added to the sample and incubated for 1 h (**Figure** 1A). If the target antigen is present in the sample, it binds to the cAb-MNPs and dually labeled AuNPs forming MNP-antigen-AuNP immunocomplexes, which are subsequently separated from the sample and washed using a magnetic rack (Figure 1B). Streptavidin-HRP is added to the solution and incubated for 10 min, resulting in HRP binding to the biotinylated detection antibody. This step increases the amount of HRP on the AuNPs, which leads to the generation of a larger electrochemical signal, thus enhancing the analytical sensitivity of the immunosensor. The MNP-antigen-AuNP immunocomplexes are then washed to remove any unbound streptavidin-HRP. 3,3',5,5'-Tetramethylbenzidine (TMB) substrate is added to the MNP-antigen-AuNP immunocomplexes, and the solution is dispensed onto a screen-printed gold electrode (SPGE) sensor. The sensor is placed on a magnetic stage (Figure S1, Supporting Information), resulting in the MNP-antigen-AuNP immunocomplexes rapidly concentrating onto the sensor surface (Figure 1C). A redox reaction between the TMB substrate and HRP on the AuNPs is generated upon application of a bias potential to the reference and working electrodes, resulting in the generation of an electrochemical signal that is proportional to the antigen concentration in the sample (Figure 1D). If there is no target antigen in the sample, no immunocomplex formation occurs between the cAb-MNPs and dually labeled AuNPs, which are subsequently washed away during magnetic separation. Thus, a negligible electrochemical signal is generated upon application of the bias potential.

Conventional immunoassays require long (1.5–3 h) incubation times for biomolecular recognition and antigen-antibody binding. Furthermore, multiple washes are required to remove unbound biomolecules and reduce nonspecific binding from the sensor surface. The use of nanoparticles (MNPs and AuNPs) in this immunosensor accelerates mass transport and enhances antigen-antibody reaction kinetics, leading to an amplified detection signal and shorter assay time. Due to their high surface area-to-volume ratio, nanoparticles can be loaded with large amounts of antibody, which facilitates biomolecular recognition and increases the likelihood of immunocomplex formation.[33,34] Additionally, the AuNPs are labeled with both HRP-conjugated detection antibody and free HRP, which has been shown to further amplify the detection signal and enhance the analytical sensitivity in a surface-binding electrochemical assay.[35]

In addition to enhancing the antigen-antibody reaction kinetics, the use of cAb-MNPs offers several additional advantages. First, the MNP-antigen-AuNP immunocomplexes can be rapidly (within minutes) concentrated onto the working electrode using an external magnet, which is significantly faster than diffusion-based mass transport. After each measurement, the MNP-antigen-AuNP immunocomplexes can be easily washed off the sensor, allowing it to be reused multiple times (Figure 1E). In this sensing scheme, the biofluid sample does not directly contact the sensing electrodes, which reduces the likelihood of nonspecific binding and interference effects due to the presence of electroactive species (e.g., uric acid and ascorbic acid) in the sample.[36,37] Furthermore, the limited time (2 min) that cAb-MNPs are in contact with the sensor reduces the likelihood that

© 2024 The Authors. Advanced Sensor Research published by Wiley-VCH GmbH

27511219, 0, Downloaded from https://onlinelibrary.wiley.com/doi/10.1002/adsr.202400004 by Rice University, Wiley Online Library on [22/04/2024]. See the Terms and Conditions (https://onlinelibrary.wiley.com/terms-and-conditions) on Wiley Online Library for rules of use; OA articles are governed by the applicable Creative Commons License

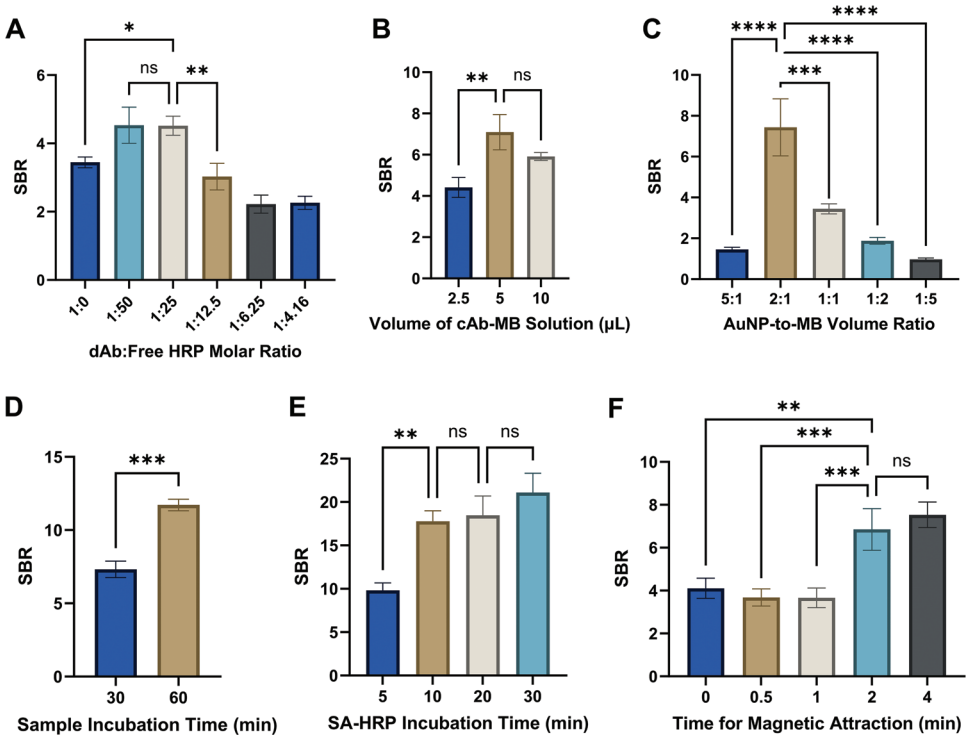

Figure 2. Optimization of Electrochemical Immunoassay Parameters. A) SBRs obtained from human urine samples spiked with CXCL9 at 0 or 10 000 pg mL^{-1} using AuNPs labeled with various dAb:HRP molar ratios. Nanoparticles were incubated with the sample for 30 min. B) SBRs obtained from CXCL9-spiked and nonspiked urine samples using varying amounts of cAb-MNPs. C) SBRs obtained from CXCL9-spiked and nonspiked urine samples using varying AuNP-to-MNP ratios. Measurements were performed using 5 µL of MNPs. D) SBRs obtained from CXCL9-spiked and nonspiked urine samples with a 30 or 60 min sample incubation period. E) SBRs obtained from CXCL9-spiked and nonspiked urine samples with varying streptavidin (SA)-HRP incubation times. F) SBRs obtained from CXCL9-spiked and nonspiked urine samples with varying times for magnetic attraction. Each bar represents the mean ± standard deviation (SD) of three independent measurements. Statistical significance was determined using a one-way ANOVA for panels A–C and E,F, and using a student's *t*-test for panel D. * indicates $p < 0.05$, ** indicates $p < 0.01$, *** indicates $p < 0.001$.

they will nonspecifically bind to the sensing electrodes, resulting in a low background signal.

2.2. Optimization of the Immunoassay Parameters

Several assay parameters were optimized to enhance the analytical sensitivity of the immunosensor and reduce the overall assay time. For every parameter that was optimized, we evaluated the signal-to-background ratio (SBR) of the assay, which was calculated using the detection signal obtained by testing a human urine sample spiked with 10 000 pg mL^{-1} of CXCL9 and the background signal obtained by testing a nonspiked urine sample. The effect of incorporating free HRP on the AuNPs was studied by performing measurements using AuNPs labeled with HRP-conjugated detection antibody only or AuNPs dually labeled with HRP-conjugated detection antibody and free HRP at varying molar ratios. Significantly larger SBRs were obtained using dually labeled AuNPs (with antibody-to-HRP molar ratios of 1:25 and 1:50) compared with AuNPs labeled only with HRP-conjugated detection antibody (**Figure** 2A). The incorporation of free HRP on the AuNPs increases the amount of HRP on each MB-antigen-AuNP immunocomplex, which leads to the oxidation of more TMB substrate and a larger electrochemical signal. We observed that the use of dually labeled AuNPs with high (≥1:6.25) antibody-to-HRP ratios resulted in low SBRs, which we attribute to a disproportionate increase in the background signal produced by the HRP-conjugated detection antibodies on the AuNPs. A 1:25 molar ratio of antibody-to-free HRP resulted in the highest SBR and the least amount of variation between replicate measurements and was selected as the optimal ratio.

The amounts of cAb-MNPs and dually labeled AuNPs incubated with the sample were optimized by performing measurements using varying volumes of cAb-MNP and AuNP solutions, which were added at a 1:2 MNP-to-AuNP volume ratio. There was a significant increase in the SBR by increasing the amount of cAb-MNP solution from 2.5 to 5 µL (Figure 2B). However, we observed no improvement in the immunosensor performance by using a larger amount (10 µL) of cAb-MNP solution, which is likely due to the sensor surface being saturated with nanoparticles. Once the sensor surface becomes fully saturated with nanoparticles, the presence of additional HRP-labeled AuNPs which are not located within the diffusion layer of the working electrode does not contribute to the redox reaction and has a negligible effect on the electrochemical signal. We also observed that using higher amounts of AuNPs relative to MNPs resulted in lower SBRs since having an abundance of HRP molecules close to the sensor surface generated a high background signal (Figure 2C). Conversely, having too many MNPs relative to

© 2024 The Authors. Advanced Sensor Research published by Wiley-VCH GmbH

27511219, 0, Downloaded from https://onlinelibrary.wiley.com/doi/10.1002/adsr.202400004 by Rice University, Wiley Online Library on [22/04/2024]. See the Terms and Conditions (https://onlinelibrary.wiley.com/terms-and-conditions) on Wiley Online Library for rules of use; OA articles are governed by the applicable Creative Commons License

AuNPs led to a reduction in the SBR due to a low amount of HRP-labeled AuNPs, resulting in minimal signal amplification and a low detection signal. Based on these results, 2:1 was selected as the optimal AuNP-to-MNP ratio.

We briefly investigated different incubation conditions and found that incubation at room temperature produced larger SBRs compared with incubation at 37 °C (Figure S2A, Supporting Information). Furthermore, there was no significant difference in the SBR when the sample was incubated with and without agitation (500 rpm), thus, static incubation at room temperature was selected as the optimal incubation condition to simplify the assay workflow and avoid the need for additional laboratory equipment (e.g., heater, shaker). The number of washes performed after magnetic separation was optimized to enhance the analytical sensitivity and simplify the assay workflow. A single wash resulted in a significant increase in the SBR compared with no washing (Figure S2B, Supporting Information) due to a decrease in the background signal. Performing > 1 wash cycle resulted in significantly lower SBRs, which we attribute to the excessive loss of cAb-MNPs.

The incubation times were optimized to maximize the analytical sensitivity while reducing the overall assay time. We first evaluated the influence of adding cAb-MNPs and dually labeled AuNPs to the sample concurrently followed by a single 30 min incubation or adding them sequentially followed by separate 30 min incubation periods. There was no significant difference in the SBR when the nanoparticles were added concurrently versus sequentially (Figure S2C, Supporting Information); therefore, we chose to add them concurrently to reduce the assay time. The sample incubation time was optimized by incubating the nanoparticles with the sample for 30 or 60 min. The longer incubation resulted in a 1.6-fold increase in the SBR (Figure 2D), and 60 min was selected as the optimal sample incubation time. Studies to optimize the streptavidin-HRP incubation time showed that 10 min resulted in a large SBR while minimizing the assay time (Figure 2E) and was selected as the optimal time. The last parameter that was optimized was the time for magnetic attraction. Incubation times ≤1 min resulted in low SBRs due to inadequate time for the MNP-antigen-AuNP immunocomplexes to migrate to the sensor surface and concentrate on the working electrode. Increasing the magnetic attraction time to 2 min resulted in a ≈2-fold increase in the SBR (Figure 2F). Incubation times >2 min resulted in a negligible improvement in the analytical performance of the immunosensor, thus, 2 min was selected as the optimal time for magnetic attraction.

2.3. Evaluation of the Immunosensor Performance

We evaluated the analytical performance of this electrochemical immunosensor by performing measurements of CXCL9 spiked in pooled human urine obtained from healthy donors. Elevated CXCL9 levels in urine have been shown to be indicative of immune-mediated kidney injury.[28,29,31] Since it is possible for CXCL9 to be present at very low levels in the urine of healthy individuals, we first measured the CXCL9 concentration in the pooled urine using a commercial ELISA kit to determine the baseline level before spiking. The CXCL9 concentration was found to be below the lower limit of detection (LOD) of the ELISA kit (Figure S3, Supporting Information), indicating that it was undetectable. Therefore, the amount of CXCL9 spiked in the pooled urine represents the actual CXCL9 concentration in the samples. Using CXCL9-spiked urine samples, calibration curves were generated for the electrochemical immunosensor with either a 30 or 60 min sample incubation. Chronoamperograms generated from the urine samples containing CXCL9 from 0 to 10 000 pg mL^{-1} show a positive correlation between the amperometric current and CXCL9 concentration (**Figure 3A**). The calibration curves produced at 30 and 60 min were both highly linear over a broad range of concentrations, with linear ranges of 0 to 10 000 pg mL^{-1} (r^2 = 0.9945) and 0 to 10 000 pg mL^{-1} (r^2 = 0.9907), respectively (Figure 3B). The lower LOD, calculated as 3× the SD at 0 pg mL^{-1} divided by the slope of the calibration curve,[38] of this immunosensor for CXCL9 detection in human urine is 302 pg mL^{-1} with a 30 min sample incubation and 27 pg mL^{-1} with a 60 min sample incubation. The analytical sensitivity of this immunosensor allows for the detection of a broad range of CXCL9 levels. The sample incubation time can be adjusted accordingly based on the anticipated CXCL9 range associated with the disease being monitored.

Measurements of CXCL9 in urine samples were performed using a benchtop potentiostat and a handheld diagnostic device, consisting of a smartphone and Sensit Smart potentiostat. A 60 min sample incubation was used for both instruments. The detection signals generated by the smartphone-based device for all tested CXCL9 concentrations were statistically similar to those generated by the benchtop potentiostat (Figure 3C). The calibration curve for the CXCL9 immunoassay generated by the smartphone-based device exhibited a highly linear response (r^2 = 0.994) from 0 to 100 000 pg mL^{-1} with a lower LOD of 65 pg mL^{-1}. These results demonstrate that the smartphone-based diagnostic device offers nearly equivalent analytical performance as the benchtop potentiostat, while offering enhanced portability for point-of-care testing. The accuracy of the electrochemical immunosensor was evaluated by performing measurements of urine samples spiked with varying concentrations of CXCL9 using the electrochemical immunosensor and a commercial ELISA kit. The CXCL9 concentrations determined using both methods are plotted in Figure 3D, which shows that the CXCL9 concentrations determined by the electrochemical immunosensor are highly correlated with those determined by the commercial ELISA kit (Pearson's correlation coefficient, r, = 0.931), indicating that the analytical performance of both assays is comparable.

2.4. Reusability of the Electrochemical Immunosensor

The reusability of this immunosensor was evaluated by performing measurements of CXCL9-spiked urine samples using fresh sensing electrodes and sensing electrodes that were reused for 100 measurements. Reused sensors were used for a total of 100 independent measurements – 50 measurements were performed with urine samples spiked with CXCL9 at 10 000 pg mL^{-1} and 50 measurements were performed with nonspiked urine samples. The low (< 15%) standard deviation across 50 independent measurements at each concentration using three separate sensors shows that this immunosensor exhibits minimal assay variability (**Figure 4A**). Furthermore, there was

© 2024 The Authors. Advanced Sensor Research published by Wiley-VCH GmbH

27511219, 0, Downloaded from https://onlinelibrary.wiley.com/doi/10.1002/adsr.202400004 by Rice University, Wiley Online Library on [22/04/2024]. See the Terms and Conditions (https://onlinelibrary.wiley.com/terms-and-conditions) on Wiley Online Library for rules of use; OA articles are governed by the applicable Creative Commons License

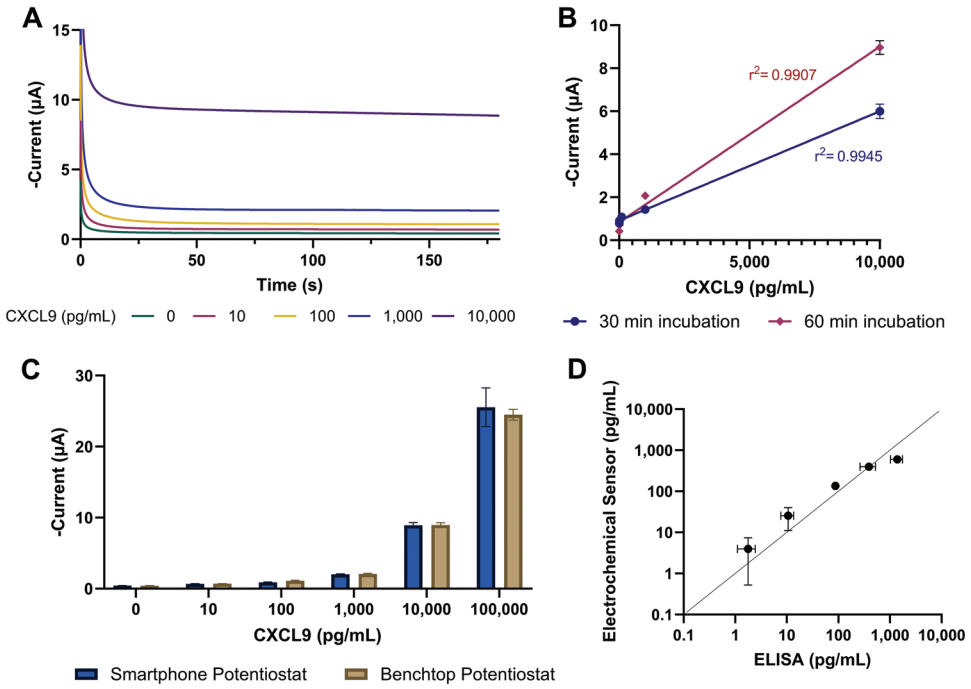

Figure 3. Analytical Performance of the Reusable Electrochemical Immunosensor. A) Chronoamperograms generated from urine spiked with CXCL9 at concentrations from 0 to 10 000 pg mL^{-1} with a 60 min incubation. Each line represents the average current produced using 3 independent measurements at each concentration. B) Calibration plots based on amperometric currents at 150 s obtained from chronoamperograms in panel A. Measurements were carried out using a benchtop potentiostat. Each point represents the mean ± SD of 3 independent measurements. C) Amperometric currents generated by the electrochemical immunosensor for measurements of urine samples spiked with CXCL9 from 0 to 100 000 pg mL^{-1} using a benchtop potentiostat and smartphone-based diagnostic device. Each bar represents the mean ± SD of three individual measurements. D) Comparison of CXCL9 concentrations in spiked urine samples determined by the electrochemical immunosensor and a commercial ELISA kit. Each data point represents the mean ± SD of 3 replicate measurements at each concentration.

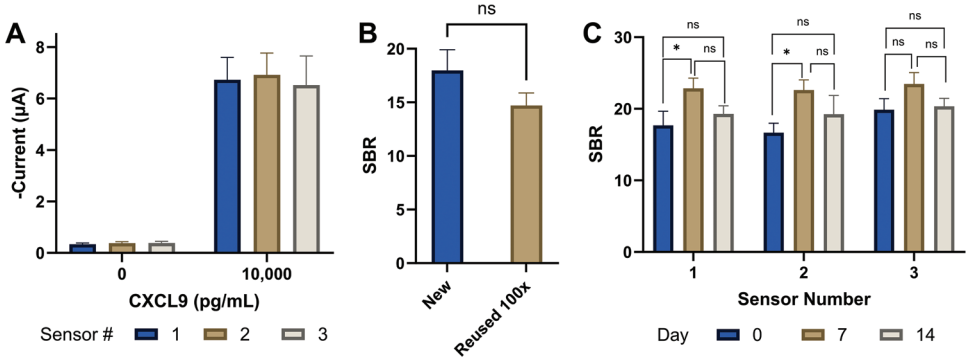

Figure 4. Reusability of the Electrochemical Immunosensor. A) Amperometric currents produced by three separate sensing electrodes at 0 and 10 000 pg mL^{-1} of CXCL9 spiked in urine. Each bar represents the mean ± SD of 50 measurements. B) SBRs obtained from urine samples spiked with CXCL9 at 0 or 10 000 pg mL^{-1} using fresh sensing electrodes and sensing electrodes reused for 100 measurements. Each bar represents the mean ± SD of 3 measurements obtained using 3 distinct sensors. Statistical significance was assessed using a student's *t*-test with significance defined as $p < 0.05$. C) SBRs obtained from urine samples spiked with CXCL9 at 0 or 10 000 pg mL^{-1} using the same sensing electrodes over the course of 14 days. Each bar represents the mean ± SD of 3 measurements. Statistical significance was assessed using a one-way ANOVA with significance defined as $p < 0.05$.

no significant difference in the SBRs obtained using the fresh sensors and those obtained using the reused sensors (Figure 4B). We further evaluated the reusability of this immunosensor by performing measurements of CXCL9-spiked urine samples using the same sensing electrodes over the course of 14 days. For this study, the sensing electrodes were stored at room temperature with desiccant and the nanoparticles were stored at 4 °C. SBRs obtained using the sensing electrodes on day 0 were similar to those obtained on day 7 and 14 with low standard deviations across 3 independent measurements (Figure 4C). The slight differences in the SBR across the timepoints are likely due to variability in the amount of CXCL9 spiked into the samples

© 2024 The Authors. Advanced Sensor Research published by Wiley-VCH GmbH

27511219, 0, Downloaded from https://onlinelibrary.wiley.com/doi/10.1002/adsr.202400004 by Rice University, Wiley Online Library on [22/04/2024]. See the Terms and Conditions (https://onlinelibrary.wiley.com/terms-and-conditions) on Wiley Online Library for rules of use; OA articles are governed by the applicable Creative Commons License

on each day. These results demonstrate that this immunosensor exhibits excellent reproducibility when reused over multiple days and can be stored at room temperature for at least 14 days with a negligible impact on the analytical performance.

While reusable electrochemical immunosensors have previously been reported,[8,10,12–17,19] most of these platforms exhibited limited reusability (< 20 uses) due to a loss of analytical performance. Furthermore, these immunosensors involved complicated regeneration strategies that make them challenging to implement in point-of-care settings. In this work, we demonstrate an electrochemical immunosensor for ultrasensitive protein measurements that maintains high analytical performance even after reusing the sensing electrodes 100 times, which is at least twofold more than previously reported reusable sensors for protein detection. Many electrochemical sensors use commercial SPGE sensors, which range in cost from $5 – $50,[39] making them cost-prohibitive for diagnostic applications requiring frequent testing or use in low- and middle-income countries. In our approach, we were able to obtain a tenfold reduction in the cost of the sensing electrode by reusing it for 100 measurements, thereby significantly reducing the cost per measurement to ≈$1.50 (Table S1, Supporting Information). In addition to reduced costs, this reusable immunosensor produces less waste compared with single-use electrochemical immunosensors.

3. Conclusion

We have developed a reusable electrochemical immunosensor for ultrasensitive measurements of protein biomarkers. This immunosensor is based on a unique sensing scheme utilizing cAb-MNPs and AuNPs dually labeled with HRP-conjugated detection antibody and HRP. The analytical performance of this immunosensor was evaluated by performing measurements of pooled human urine spiked with CXCL9, which could be detected at concentrations as low as 27 pg mL^{-1} within ≈1 h. This immunosensor was also adapted for a smartphone-based diagnostic device, which exhibited a lower LOD of 65 pg mL^{-1}. We demonstrate that sensing electrodes can be reused for at least 100 measurements with a negligible loss in analytical performance. The high analytical performance, portability and low cost (≈$1.50 per test) of this immunosensor makes it a promising diagnostic tool for use in point-of-care settings and diagnostic testing in low- and middle-income countries. Furthermore, the quantification of CXCL9 in urine can be used to differentiate the cause of kidney injury, enabling earlier diagnosis in treatable medical conditions, such as renal allograft rejection[28-30] or acute interstitial nephritis from immunotherapy or other drugs.[31,32] The use of CXCL9 for proof of principle demonstrates the functionality of this platform. Based on other immunoassays that we have developed employing dually labeled nanoparticles for high sensitivity protein measurements in blood and blood-derived fluids,[35,40,41] we envision that this reusable electrochemical immunosensor can be adapted for the detection of other protein biomarkers in other biofluids (e.g., blood, serum, plasma) by modifying the capture and detection antibodies bound to the nanoparticles and optimizing the immunoassay parameters (e.g., incubation time), ultimately expanding the utility of this platform for diagnostic testing.

4. Experimental Section

Biochemicals and Reagents: 0.1 M 2-(N-morpholino) ethanesulfonic acid (MES, pH = 4.7) and N-(3-dimethylaminopropyl)-N-ethylcarbodiimide (EDC) were purchased from Thermo Fisher Scientific. Tween-20 (Sigma-Aldrich) was diluted in phosphate buffered saline (PBS) (Sigma-Aldrich) to obtain a 0.05% solution for washing. 30 nm OD1 AuNPs, N-hydroxysuccinimide (NHS), protease-free bovine serum albumin (BSA), HRP and TMB substrate were purchased from Sigma-Aldrich. StabilZyme SELECT stabilizer and StabilZyme HRP stabilizer were purchased from Surmodics IVD (Eden Prairie, MN). Streptavidin-HRP, anti-CXCL9 IgG capture antibody, biotinylated anti-CXCL9 IgG detection antibody and recombinant human CXCL9 protein were purchased from R&D Systems (Minneapolis, MN). Proteins were reconstituted in sterile PBS and stored at −20 °C until use. Pooled human urine from two or more healthy donors was purchased from Innovative Research (Novi, MI) and stored at −20 °C until use. All human samples were de-identified of all identifying information.

Preparation of Magnetic Nanoparticles: 200 nm carboxyl functionalized MNPs (Ademtech, France) were conjugated to anti-CXCL9 IgG using EDC/NHS functionalization as previously described.[35,40] Briefly, 1 mg of MNPs was washed with 25 mM MES (pH 5.5–6) and activated with 100 µL of 20 mg mL^{-1} NHS and 100 µL of 20 mg mL^{-1} EDC reconstituted in MES for 1 h. Magnetic separation was used to remove the excess EDC and NHS and wash the MNPs with MES. 10 µg of anti-CXCL9 capture antibody was added to the MNPs and incubated for 16–20 h with shaking. Following incubation, the unbound protein was washed off using PBS, and the MNPs were blocked with 400 µL of 3% BSA solution in PBS for 90 min to prevent nonspecific binding. The MNPs were washed with PBS and stored in StabilZyme SELECT stabilizer at 4 °C until use.

Preparation of Dually Labeled AuNPs: 30 nm OD1 AuNPs were labeled with biotinylated anti-CXCL9 IgG and HRP, as previously reported.[42] Briefly, 1 mL of AuNP solution was spun down at 12 000 ×g for 10 min to pellet the AuNPs. Two-thirds of the supernatant was removed, and the AuNPs were resuspended in the remaining ≈330 µL of buffer. 5 µL of anti-CXCL9 IgG (200 µg mL^{-1}) and 8 µL of HRP (1 mg mL^{-1}) were added to the AuNPs and incubated with shaking at 500 rpm for 3 h. After incubation, 10 mg of BSA was added to the suspension and incubated for 1 h with shaking at 500 rpm to block unbound sites on the AuNP surface. The AuNP suspension was then centrifuged at 12 000×g for 15 min and the supernatant was removed. The dually labeled AuNPs were reconstituted in 200 µL of StabilZyme HRP stabilizer and stored at 4 °C until use.

Preparation of SPGE Sensors: Electrochemical measurements were performed using SPGE sensors with a 4 mm-diameter working electrode (Metrohm AG, Switzerland). A 0.9 cm-diameter circular ring was cut out of polymethyl methacrylate (PMMA) (McMaster Carr, Elmhurst, IL) using a CO_2 laser cutter and attached to the sensor using double-sided adhesive tape (Adhesive Research, Glen Rock, PA) to confine the liquid sample over the sensing electrodes.

Design and Fabrication of the Magnetic Stage: The magnetic stage consists of a rectangular opening to hold the SPGE sensor and a 3.175 mm-diameter neodymium magnet (McMaster Carr) positioned under the working electrode (Figure S1, Supporting Information). The stage was laser cut out of PMMA and the magnet was secured using double-sided tape.

Electrochemical Measurements: 5 µL of cAb-MNP solution and 10 µL of dually labeled AuNP solution were added to 100 µL of human urine spiked with CXCL9 and incubated for 30 or 60 min. The MNP-antigen-AuNP immunocomplexes were separated using a magnetic rack (Sigma-Aldrich) and washed in MES to remove unbound nanoparticles. 100 µL of 1× streptavidin-HRP was then added to the solution, incubated for 10 min, and MNP-antigen-AuNP immunocomplexes were separated and washed using a magnetic rack. 100 µL of TMB substrate was added to the MNP-antigen-AuNP immunocomplexes and the solution was dispensed onto the sensor, which was placed on the magnetic stage. After 2 min, chronoamperometric measurements were performed using a PalmSens4 potentiostat (PalmSens BV, Netherlands) or smartphone-based Sensit Smart potentiostat (PalmSens) by applying a bias potential of −0.2 V (vs

© 2024 The Authors. Advanced Sensor Research published by Wiley-VCH GmbH

27511219, 0, Downloaded from https://onlinelibrary.wiley.com/doi/10.1002/adsr.202400004 by Rice University, Wiley Online Library on [22/04/2024]. See the Terms and Conditions (https://onlinelibrary.wiley.com/terms-and-conditions) on Wiley Online Library for rules of use; OA articles are governed by the applicable Creative Commons License

Ag/AgCl) for 160 s. Current values were obtained at 150 s of chronoamperograms. For the study comparing the analytical performance of the electrochemical immunosensor with ELISA, a scaling factor of 0.12 was applied to the CXCL9 concentrations determined by the electrochemical immunosensor to account for the differences in the detection signals generated by both methods.

Immunosensor Reusability Testing: Immunosensor reusability was evaluated by testing human urine samples spiked with CXCL9 at 0 or 10 000 pg mL^{-1} using the same sensing electrodes for up to 100 measurements. After each measurement, the sensing electrodes were gently rinsed with 0.05% Tween 20 in PBS for 10 s using a squeeze bottle and dried using compressed air. Sensing electrodes were stored at room temperature with desiccant between measurements. For these studies, cAb-MNPs and dually labeled AuNPs were prepared at the start of the experiment and stored at 4 °C, and the same batch of nanoparticles was used for all measurements.

ELISA Measurements: Measurements of CXCL9-spiked urine samples were performed using a CXCL9 ELISA kit (R&D Systems). Measurements were performed according to the manufacturer's instructions and absorbance values were measured at OD 450 and OD 570 using a BioTek Epoch microplate spectrophotometer. The OD 450 – OD 570 value was used as the final absorbance value for analysis.

Statistical Analysis: All data was run in triplicates and analyzed using means and standard deviation. The SBR was calculated by dividing the detection signal generated by the immunosensor for a CXCL9-spiked urine sample by the signal generated for a nonspiked urine sample. Error was propagated from the standard deviations of the positive and negative signals to determine the standard deviations of the SBRs. Statistical analysis was conducted using a two-tailed Student's *t*-Test or a one-way ANOVA with a post-hoc Tukey's comparison. Correlation was assessed using Pearson's correlation coefficient. Statistical significance was defined as $p < 0.05$. Data analysis was conducted using Microsoft Excel and GraphPad Prism 10.

Supporting Information

Supporting Information is available from the Wiley Online Library or from the author.

Acknowledgements

This work was supported in part by the National Institutes of Health (R21AI171477 and K08DK119466).

Conflict of Interest

The authors declare no conflict of interest.

Data Availability Statement

The data that support the findings of this study are available from the corresponding author upon reasonable request.

Keywords

CXCL9, diagnostic, electrochemical, gold nanoparticles, immunosensor, magnetic nanoparticles, reusable

Received: January 13, 2024
Revised: March 29, 2024
Published online:

[1] H. Hayrapetyan, T. Tran, E. Tellez-Corrales, C. Madiraju, *Enzyme-Linked Immunosorbent Assay: Types and Applications*, Springer US, New York, **2023**
[2] A. Erdem, H. Senturk, E. Yildiz, M. Maral, *Talanta* **2022**, *244*, 123422.
[3] E. Akyilmaz, E. Dinçkaya, *Artif. Cells Nanomed. Biotechnol.* **2013**, *41*, 389.
[4] C. Zhou, D. Liu, L. Xu, Q. Li, J. Song, S. Xu, R. Xing, H. Song, *Sci. Rep.* **2015**, *5*, 9939.
[5] A. Lomae, P. Preechakasedkit, O. Hanpanich, T. Ozer, C. S. Henry, A. Maruyama, E. Pasomsub, A. Phuphuakrat, S. Rengpipat, T. Vilaivan, O. Chailapakul, N. Ruecha, N. Ngamrojanavanich, *Talanta* **2023**, *253*, 123992.
[6] J. Su, S. Chen, Y. Dou, Z. Zhao, X. Jia, X. Ding, S. Song, *Anal. Chem.* **2022**, *94*, 3235.
[7] S. S. Shi, X. J. Li, R. N. Ma, L. Shang, W. Zhang, H. Q. Zhao, L. P. Jia, H. S. Wang, *Lab Chip* **2024**, *24*, 367.
[8] Y. Yang, Y. Huang, C. Li, *Anal. Chim. Acta* **2019**, *1055*, 90.
[9] Z.-S. Wu, M.-M. Guo, S.-B. Zhang, Chen, J.-H. Jiang, G.-L. Shen, R.-Q. Yu, *Anal. Chem.* **2007**, *79*, 2933.
[10] W. Hong, S. Lee, E. Jae Kim, M. Lee, Y. Cho, *Biosens. Bioelectron.* **2016**, *78*, 181.
[11] Z. Panahi, M. A. Merrill, J. M. Halpern, *ACS Appl. Polym. Mater.* **2020**, *2*, 5086.
[12] G.-J. Yang, J.-L. Huang, W.-J. Meng, M. Shen, X.-A. Jiao, *Anal. Chim. Acta* **2009**, *647*, 159.
[13] W. Limbut, P. Kanatharana, B. Mattiasson, P. Asawatreratanakul, P. Thavarungkul, *Anal. Chim. Acta* **2006**, *561*, 55.
[14] J. Wu, J. He, Y. Zhang, Y. Zhao, Y. Niu, C. Yu, *Microchim. Acta* **2017**, *184*, 1837.
[15] X. Zhang, Y. Wu, Y. Tu, S. Liu, *Analyst* **2008**, *133*, 485.
[16] S. Liu, X. Zhang, Y. Wu, Y. Tu, L. He, *Clin. Chim. Acta* **2008**, *395*, 51.
[17] S. Xiao, X. Yang, J. Wu, Q. Liu, D. Li, S. Huang, H. Xie, Z. Yu, N. Gan, *Sens. Actuators, B* **2022**, *369*, 132320.
[18] Y. Zhang, H. Wang, B. Yan, Y. Zhang, J. Li, G. Shen, R. Yu, *J. Immunol. Methods* **2008**, *332*, 103.
[19] R. Chauhan, J. Singh, P. R. Solanki, T. Basu, R. O'Kennedy, B. D. Malhotra, *Biochem. Eng. J.* **2015**, *103*, 103.
[20] H. Wang, D. Li, Z. Wu, G. Shen, R. Yu, *Talanta* **2004**, *62*, 199.
[21] P. Ding, R. Liu, S. Liu, X. Mao, R. Hu, G. Li, *Sens. Actuators, B* **2013**, *188*, 1277.
[22] M. Salmain, M. Ghasemi, S. Boujday, C.-M. Pradier, *Sens. Actuators, B* **2012**, *173*, 148.
[23] C. Huang, Z. Hao, T. Qi, Y. Pan, X. Zhao, *J. Materiomics* **2020**, *6*, 308.
[24] T. W. Lin, P. J. Hsieh, C. L. Lin, Y. Y. Fang, J. X. Yang, C. C. Tsai, P. L. Chiang, C. Y. Pan, Y. T. Chen, *Proc. Natl. Acad. Sci. U. S. A.* **2010**, *107*, 1047.
[25] E. Kang, J.-W. Park, S. J. McClellan, J.-M. Kim, D. P. Holland, G. U. Lee, E. I. Franses, K. Park, D. H. Thompson, *Langmuir* **2007**, *23*, 6281.
[26] X. Duan, L. Mu, S. D. Sawtelle, N. K. Rajan, Z. Han, Y. Wang, H. Qu, M. A. Reed, *Adv. Funct. Mater.* **2015**, *25*, 2279.
[27] J. Jun, J. S. Lee, D. H. Shin, J. Jang, *ACS Appl. Mater. Interfaces* **2014**, *6*, 13859.
[28] S. Schaub, P. Nickerson, D. Rush, M. Mayr, C. Hess, M. Golian, W. Stefura, K. Hayglass, *Am. J. Transplant.* **2009**, *9*, 1347.
[29] D. E. Hricik, P. Nickerson, R. N. Formica, E. D. Poggio, D. Rush, K. A. Newell, J. Goebel, I. W. Gibson, R. L. Fairchild, M. Riggs, K. Spain, D. Ikle, N. D. Bridges, P. S. Heeger, *Am. J. Transplant.* **2013**, *13*, 2634.
[30] J. A. Jackson, E. J. Kim, B. Begley, J. Cheeseman, T. Harden, S. D. Perez, S. Thomas, B. Warshaw, A. D. Kirk, *Am. J. Transplant.* **2011**, *11*, 2228.
[31] S. Singh, J. P. Long, A. Tchakarov, Y. Dong, C. Yee, J. S. Lin, *JCI Insight* **2022**, e165108, https://doi.org/10.1172/jci.insight.165108.

© 2024 The Authors. Advanced Sensor Research published by Wiley-VCH GmbH

27511219, 0, Downloaded from https://onlinelibrary.wiley.com/doi/10.1002/adsr.202400004 by Rice University, Wiley Online Library on [22/04/2024]. See the Terms and Conditions (https://onlinelibrary.wiley.com/terms-and-conditions) on Wiley Online Library for rules of use; OA articles are governed by the applicable Creative Commons License

[32] D. G. Moledina, W. Obeid, R. N. Smith, I. Rosales, M. E. Sise, G. Moeckel, M. Kashgarian, M. Kuperman, K. N. Campbell, S. Lefferts, K. Meliambro, M. Bitzer, M. A. Perazella, R. L. Luciano, J. S. Pober, L. G. Cantley, R. B. Colvin, F. P. Wilson, C. R. Parikh, *J. Clin. Invest.* **2023**, *133*, e168950.
[33] I.-H. Cho, J. Lee, J. Kim, M.-S. Kang, J. K. Paik, S. Ku, H.-M. Cho, J. Irudayaraj, D.-H. Kim, *Sensors (Basel, Switzerland)* **2018**, *18*, 207.
[34] M. Li, P. Wang, F. Li, Q. Chu, Y. Li, Y. Dong, *Biosens. Bioelectron.* **2017**, *87*, 752.
[35] J. Li, P. B. Lillehoj, *ACS Sens.* **2021**, *6*, 1270.
[36] S. Pradhan, S. Albin, R. L. Heise, V. K. Yadavalli, *Chemosensors* **2022**, *10*, 263.
[37] G. Dutta, P. B. Lillehoj, *Sci. Rep.* **2018**, *8*, 17129.
[38] D. C. Harris, *Quantitative Chemical Analysis*, W.H. Freeman and Co., New York, **2007**
[39] K. Partanen, D. S. Lee, A. Omoboye, K. McEleney, R. X. Y. Chen, Z. She, *J. Electrochem. Soc.* **2023**, *170*, 092510.
[40] K. L. Singampalli, J. Li, P. B. Lillehoj, *Anal. Chim. Acta* **2022**, *1225*, 340246.
[41] J. Li, P. B. Lillehoj, *Angew. Chem., Int. Ed.* **2022**, *61*, e202200206.
[42] X. Jiang, P. B. Lillehoj, *Microsyst. Nanoeng.* **2020**, *6*, 96.

© 2024 The Authors. Advanced Sensor Research published by Wiley-VCH GmbH

27511219, 0, Downloaded from https://onlinelibrary.wiley.com/doi/10.1002/adsr.202400004 by Rice University, Wiley Online Library on [22/04/2024]. See the Terms and Conditions (https://onlinelibrary.wiley.com/terms-and-conditions) on Wiley Online Library for rules of use; OA articles are governed by the applicable Creative Commons License